Investigation of Drag and Heat Transfer for Martian Dust Particles

T. Ozawa, T. Suzuki, H. Takayanagi, and K. Fujita

*Aerospace Research and Development Directorate
Japan Aerospace Exploration Agency,
Chofu, Tokyo 182-8522 JAPAN*

Abstract. A Mars non-stop dust sample return project has been going on in a Mars exploration mission at Japan Aerospace Exploration Agency. In the project, sampling of Martian dust particles is planned between 35 and 45 km, and thus, the survivability of micron-size particles during traveling through a hot-temperature shock is crucial. In this work, the dust particle heating was investigated from macroscopic and microscopic viewpoints. Drag and heat transfer coefficients calculated by the direct simulation Monte Carlo method were found to agree well with Koshmarov and Svirshevskii and free-molecule models at both altitudes, and particle heating estimations calculated by these models were validated.

Keywords: Mars, Dust, Heat Transfer, Martian Atmosphere, DSMC, MASC

INTRODUCTION

At Japan Aerospace Exploration Agency (JAXA), the Mars Exploration with Lander-Orbiter Synergy (MELOS) mission has come under review together with a lot of planetary scientific groups all over Japan. As one of the MELOS projects, a non-stop Mars sample return project, named Mars Aero-flyby Sample Collection (MASC) [1, 2], has been planned in our group. In order to improve the feasibility of this project, investigation of the effect of a hot-temperature shock to micron-size dust particles is crucial [3, 4]. In our previous work [5], the Martian dust distributions were examined [6], and it was found that there are a plenty of micron size dust particles between 30 and 50 km altitude depending on the weather condition, where the dust sampling is planned for the MASC project. The computational fluid dynamics (CFD) and direct simulation Monte Carlo (DSMC) [7] flow field calculations were performed for a sphere-cone shape spacecraft [8] entry in the Martian atmosphere at 35 and 45 km altitudes. For the estimation of the Martian dust heating when dust particles travel through the hot-temperature shock, particle motion, heat transfer, and thermal decomposition were simulated. In the high-temperature rarefied, low-Reynolds number conditions from subsonic to supersonic, three macroscopic heat transfer models, the modified Kavanau [9], Koshmarov and Svirshevskii (K-S) [10], and free-molecule (F-M) [11] models, were compared. It was found that the difference between K-S and F-M models was small in the dust sample conditions, and these models predicted the higher particle temperature in the stagnation region than the modified Kavanau model. However, in the downstream region, the modified Kavanau model predicted higher particle temperature than the other two models. The maximum particle temperature was approximately 740 K and 525 K at 35 and 45 km, respectively, using the K-S or F-M model. In this work, in order to verify the accuracy of the macroscopic models, the drag coefficient C_D [12, 13] and the heat transfer coefficient C_h of macroscopic models in the dust particle simulations were compared with the microscopic DSMC results.

DRAG AND HEAT TRANSFER IN DSMC

In order to investigate the influence of a hot-temperature shock on the micron-size dust particles, Mars atmosphere entry flow fields and the shock structures need to be obtained at descent altitudes for the dust sampling, and thus in this work, 2D-axisymmetric CFD and DSMC computations have been performed at 35 and 45 km altitudes. Free stream conditions, such as the total number density, temperature, speed and mole fractions of each species, at 35 and 45 km for the Mars entry are listed in Table 1. As shown in the table, the number density at 45 km is considerably lower than the 35 km case, and the continuum assumption may not be applicable for the hypersonic bow-shock flows at this altitude due to the breakdown effect. Therefore, the DSMC particle simulations have been carried out for the 45 km case instead of the continuum method while 2D axisymmetric CFD calculations have been performed at 35 km. The details of the CFD modeling can be found in Ref. [14] and [5]. At JAXA, a new DSMC code, named modeling of transitional-ionized flows (MOTIF), has been developed, and this code has been used for the flow field calculations at 45 km and the microscopic drag and heat transfer calculations. 8 species (N, O, C, N_2, O_2, NO, CO, CO_2) were considered for the Mars entry calculations. Note that the details of the DSMC code can be found in Ref. [5] and [15].

TABLE 1. Mars entry conditions

Altitude	35 km	45 km
n_∞, m^{-3}	5.8452×10^{21}	1.6×10^{21}
T_∞, K	171	152.67
v_∞, km/s	4.194	5.0
CO_2	0.967	0.971
N_2	0.027	0.027
Ar	0.016	0.0
O_2	0.0	0.0017
CO	0.0	0.0007

For the investigation of drag and heat transfer coefficients in the flow regime specified in Fig. 2, the results obtained by the macroscopic models are compared with microscopic DSMC results. In DSMC, the drag force and heat transfer are calculated microscopically as follows. The drag force F_D is calculated from the summation of particle momentum transfer as

$$F_D = \sum_p \left[(mv_{x,p}^{pre} - mv_{x,p}^{post}) F_{num,p} \right] / \Delta t, \tag{1}$$

where m and $v_{x,p}$ are the molecular mass and the velocity component in the x-direction, respectively. Note that the free stream direction is set to the x-direction. $F_{num,p}$ is the number of real molecules represented by a single DSMC molecule. The superscripts, pre and post, denote the pre-collisional and post-collisional properties. The heat transfer rate q is calculated from the summation of particle energy transfer as

$$q = \sum_p \left[(E_{col,p}^{pre} - E_{col,p}^{post}) F_{num,p} \right] / \Delta t, \tag{2}$$

where $E_{col,p}$ is the particle collisional energy. The particle information was accumulated over the sampling time steps and the F_D and q are the average value over the sampling time to reduce the statistical noise. The non-dimensional drag and heat transfer coefficients are calculated as follows.

$$\begin{aligned} C_D &= \frac{F_D}{(\rho_\infty U_\infty^2/2) \times \pi r_d^2}, \\ C_h &= \frac{q}{(\rho_\infty U_\infty^3/2) \times \pi d_d^2}, \end{aligned} \tag{3}$$

where ρ_∞ and U_∞ are the free stream density and speed, respectively. r_d and d_d are the radius and diameter of a dust particle. The overall C_D and C_h are calculated in DSMC and compared with the macroscopic models.

RESULTS AND DISCUSSION

Investigations of Drag and Heat Transfer Coefficients at 35 km

Particle motion, heat transfer, and thermal decomposition of a micron-size Martian dust were simulated using the three macroscopic models, Kavanau, K-S and F-M models, in the Mars entry flow field at 35 km. The heating of dust particles in the stagnation region is presented in Fig. 3 as a function of time in the Mars atmosphere entry flow field at 35 km. The accommodation coefficient of the dust particle surface is set to unity for the calculations in Fig. 3. Based on the Martian dust size distributions, the most plausible particle size to be sampled is between 1 and 2 μm. Thus, 1 μm-, 2 μm-size dust particles are investigated, and in case that the larger particle is sampled, a 10 μm-size dust particle is also compared. Inside a shock, particle temperature gradually increases, and the increase rate is higher for the smaller particle. Temperatures of 1, 2, and 10 μm-size dust particles reach at approximately 660, 450 and 250 K, respectively, using the modified Kavanau model when the particles are captured on the body. The difference between the K-S and F-M models is small, and using these models the maximum temperatures for 1, 2, and 10 μm-size dust particles are roughly 740, 500 and 260 K, respectively. The temperature increase is the maximum in the stagnation region, and the temperature change is smaller when the particle trajectory goes farther away from the axisymmetric line as is shown in Fig. 4. For trajectories (1)-(3), the initial r coordinate is 0, 30 and 50 cm, respectively. Note that although the modified Kavanau model predicts the lowest particle temperature for trajectory (1), the difference is small among three models for trajectory (2) and the modified Kavanau model predicts the highest particle temperature for trajectory (3). This is because the K-S model is more sensitive to the change of the Reynolds number Re. Since the decrease of Re is more significant from the stagnation to the downstream region than the Mach number, the relation among three models was also changed dramatically from the stagnation to downstream. The decrease of the Nusselt number Nu is more prominent in the K-S and F-M models from the stagnation to the downstream, the heating prediction of these two models became lower than the Kavanau model for trajectory (3) in contrast to the higher heating prediction in the stagnation region.

In order to investigate the reliability of macroscopic models, the drag and heat transfer coefficients were compared with the microscopic DSMC computations for the rarefied supersonic flow regime. Along the trajectories (1) and (3), two typical flow conditions (one is away from the body and a lower density and another is near the body and a higher density) were chosen, and 2D-axisymmetric DSMC calculations were performed. The selected coordinates and the flow conditions are listed in Table 2. The relative velocity, temperature, and total number density as well as mole fractions of each species are obtained for the DSMC calculations. For cases (1) and (2) on the trajectory (1), the Knudsen number Kn is lower than 5 and the Mach number M is approximately 4 because of the low flow velocity in the stagnation region. For cases (3) and (4) on the trajectory (3), Kn is higher than 10 and M is approximately 2. By simulating flows around a sphere, C_D and C_h on the sphere were calculated for each flow condition. A dust radius of 1 μm for the sphere and the accommodation coefficient of 1.0 were used for the DSMC drag and heat transfer computations. First of all, it is noteworthy that C_D obtained by the DSMC calculations agrees well with the macroscopic results for all of the flow conditions. Secondly, the DSMC heat transfer coefficients agrees well with the K-S and F-M models for cases (1) and (2). While the discrepancy between the Kavanau model and the DSMC is not large for case (1), it is increased for case (2). These results accord with the particle temperature prediction for trajectory (1) shown in Fig. 3. For cases (3) and (4), because the Kn is so high that the C_h(DSMC) agrees with the F-M model the best and the K-S model predicts slightly lower than the DSMC. The Kavanau model predicts considerably higher C_h than the other three results, and thus, the Kavanau model predicts the highest particle temperature for trajectory (3). Furthermore, the effect of gas mixture in the DSMC calculations is found to be so small that the macroscopic calculations using the CO_2 properties are able to predict the particle heat transfer well. In summary, since the DSMC results are basically between the K-S and F-M models and these models predict similar particle temperature, these two models are more reliable than the Kavanau model at 35 km.

TABLE 2. Drag and heat transfer coefficients at 35 km

Parameter	Case(1)	Case(2)	Case(3)	Case(4)
t, s	4.01×10^{-6}	6.01×10^{-6}	2.00×10^{-5}	6.00×10^{-5}
x, m	-1.20×10^{-2}	-4.14×10^{-3}	4.41×10^{-1}	5.82×10^{-1}
M	3.92	4.24	2.15	2.20
Re	0.55	0.72	8.52×10^{-2}	4.82×10^{-2}
ρ, kg/m^3	8.42×10^{-3}	9.83×10^{-3}	1.99×10^{-3}	1.11×10^{-3}
v_R, m/s	3839.5	3887.6	1495.24	1954.2
T_d, K	410	632	264	411
Kn(L=2 μm)	3.1	2.69	13.26	23.7
C_D(Macro)	2.32	2.32	2.87	2.77
C_D(DSMC)	2.34	2.34	2.85	2.85
C_h(Kavanau)	0.42	0.36	1.12	0.93
C_h(K-S)	0.43	0.39	0.86	0.77
C_h(F-M)	0.45	0.41	0.91	0.81
C_h(DSMC)	0.44	0.40	0.91	0.82

Investigations of Drag and Heat Transfer Coefficients at 45 km

Similar to 35 km, dust particle motion, heat transfer, and thermal decomposition were simulated in the Mars entry flow field at 45 km. A rarefaction effect can be more important at this altitude than 35 km, and in the same way as the 35 km case, three heat transfer models were compared and discussed. At this altitude, M based on the relative velocity is between 3 and 4 inside the shock. C_D is approximately 2.3 inside the shock, and C_D is only slightly higher for a 1-μm particle than that for a 2-μm particle. In Fig. 5, temperature increases of dust particles along the stagnation line are compared among the modified Kavanau, K-S ($\alpha = 1.0$) and F-M ($\alpha = 1.0$) models for 1, 2, and 10 μm-size dust particles. Inside the shock, the dust particle temperature gradually increases, and the heating rate is higher for the smaller particle. Using the modified Kavanau model, temperatures of the 1, 2 and 10 μm-size particles reach at approximately 456, 328 and 192 K, respectively, when the particles are captured on the body. Using the K-S model with $\alpha = 1.0$, these temperatures are approximately 526, 372 and 208 K, and the difference between the K-S and F-M models is small. The difference between the Kavanau and K-S models is comparatively large, which is 70 K at most, and it is less than 10 K between the K-S and F-M models. These temperatures are lower than the 35 km case because of the lower density and lower heat transfer rate. In fact, compared to the case of 35 km, the maximum temperature for a 1 μm dust particle predicted by these models is decreased by roughly 200 K. Note that the particle simulations were also carried out in the downstream region, and similar features to the 35 km case were obtained. The K-S and F-M models predict a higher heating rate than the modified Kavanau model in the stagnation region, and as a dust particle goes downstream, the heating rate is decreased especially using the K-S and F-M models, and finally these two models predict lower particle temperature than the Kavanau model. This phenomenon is due to the lower sensitivity of the Kavanau model to the variance of *Re*.

Drag and heat transfer coefficients were compared with the microscopic DSMC results for the rarefied supersonic flow condition at 45 km, and the reliability of three macroscopic models was investigated in the stagnation region. Along the trajectory (1), three typical flow conditions were chosen and the selected coordinates and the flow conditions are listed in Table 3. The *Kn*, *M* and *Re* significantly change during traveling through the shock along the trajectory, and thus, the prediction of macroscopic models may be influenced by the flow condition transition. For case (1), the flow is in a supersonic, rarefied flow regime, where *Kn* is higher than 10, *Re* is lower than 0.1, and *M* is approximately 3.6. For case (2), *Kn* is lower than 10, and *M* and *Re* are roughly 4.8 and 0.22, respectively. Case (3) is near the body, and *Kn* is considerably decreased, which is around 2.2. *M* and *Re* are approximately 8 and 1.7, respectively. For each condition, 2D-axisymmetric DSMC computations were carried out to simulate flows over a 1 μm radius sphere to calculate the C_D and C_h. To start with, it is worth noting that good agreement on C_D is obtained between the macroscopic and DSMC results for all the cases. For case (1), with respect to C_h, good agreement is also found between the macroscopic and DSMC results, although the K-S model predicts a slightly lower value. For case (2), the C_h obtained by the DSMC agrees well with both of the K-S and F-M models. However, the Kavanau model predicts the lowest C_h. For case (3), similar feature to case (2) is observed. Nevertheless, the discrepancy between the Kavanau model and other results is increased. All in all, it is found that the DSMC results agree well with the K-S and F-M models, and the Kavanau model predicts the lower heat transfer rate. This corresponds to the particle temperature results in Fig. 5.

TABLE 3. Drag and heat transfer coefficients at 45 km

Parameter	Case (1)	Case (2)	Case (3)
t, s	4.22×10^{-6}	6.02×10^{-6}	6.92×10^{-6}
x, m	-0.014	-0.005	-6.2×10^{-4}
M	3.58	4.75	8.06
Re	0.085	0.22	1.697
v_R, m/s	4768.3	4931.73	4926.98
Kn(*L*=2 μm)	14.8	8.94	2.23
C_D(Macro)	2.339	2.231	2.130
C_D(DSMC)	2.329	2.252	2.08
C_h(Kavanau)	0.50	0.34	0.173
C_h(K-S)	0.46	0.36	0.26
C_h(F-M)	0.51	0.39	0.27
C_h(DSMC)	0.50	0.38	0.26

CONCLUSIONS

The feasibility of capturing micron-size Martian dust particles for a Mars non-stop dust sample return project has been investigated in this work. The effect of a hot-temperature shock to micron-size dust particles was estimated by simulating particle motion, heat transfer, and thermal decomposition. Moreover, the heat transfer rates were examined by comparing between three macroscopic models and microscopic calculations. CFD and DSMC flow field calculations were performed for a spacecraft entry in the Martian atmosphere at 35 and 45 km altitudes, and in the flow fields, three macroscopic heat transfer models, the modified Kavanau, K-S, and F-M models, were compared for the estimation of Martian dust heating when dust particles travel through the hot-temperature shock. It was found that the discrepancy between K-S and F-M models is small in the dust sample conditions, and these two models predict higher particle temperature in the stagnation region than the modified Kavanau model. On the contrary, in the downstream region, the modified Kavanau model predicts higher particle temperature since this model is less sensitive to the variance of *Re* compared to the other two models. The maximum dust particle temperature at 35 km is observed in the stagnation region and is approximately 740 K using the K-S and F-M models for a 1 μm particle. At 45 km, the maximum T_d is only 530 K even in the stagnation region. Furthermore, the reliability of macroscopic models in the rarefied, low *Re*, supersonic to hypersonic flow regime were discussed by being compared with the microscopic DSMC calculations. To sum up the major characteristics, the macroscopic drag coefficients are in good agreement with the DSMC results at both altitudes, and the K-S and F-M models agree better with the DSMC than the Kavanau model for C_h. In the downstream region, the K-S and F-M models predict lower heat transfer rates than the Kavanau model and the influence of a hot-temperature shock is lower, and therefore, it is suitable to sample micron-size dust particles in the rear region. Also, since the thermal decomposition effect is found to be negligibly small, the micron-size dust particle sampling at these altitudes is feasible and the dust constituents may not be destroyed during the traveling through the shock. It should be noted that heating and sublimation of dust particles in a capturing medium, such as silica aerogel, need to be considered for the overall evaluation, and in our future work, the effect of an aerogel impact and heating during a penetration of an aerogel is planned to be investigated by hypervelocity impact experiments.

REFERENCES

1. Fujita, K., Tachibana, S., Sugita, S., Miyamoto, H., Mikouchi, T., Suzuki, T., Takayanagi, H., Ozawa, T., Kawaguchi, J., and Woo, H., "Preliminary Study of Nonstop Mars Sample Return System Using Aerocapture Technologies," AIAA paper 2009-5614, AIAA Atmospheric Flight Mechanics Conference, Chicago, Illinois, August 10 - 13, Aug. 2009.
2. Fujita, K., Kubota, T., Ogawa, J., Yano, M., Suzuki, T., Takayanagi, H., Yamada, T., and Kawaguchi, J., "Assessment of Aeroassist Orbital Maneuver Technologies for Next Mars Exploration," ISTS paper 2009-k-25, 27th International Symposium on Space Technology and Science, Tsukuba, Ibaraki, JAPAN, July 5-12, July 2009.
3. Leshin, L. A., Yen, A., Clark, B., Forney, L., Gamber, T., Jones, S., Jurewicz, A., Richardson, M., Sharp, T., Thiemens, M., and Zolensky, M., "Sample Collection for Investigation of Mars (SCIM): Study of an Early Mars Sample Return Mission Through the Mars Scout Program," *Meteoritics and Planetary Science Supplement*, Vol. 36, Sept. 2001, pp. 113–+.
4. Jurewicz, A. J. G., Forney, L., Bomba, J., Vicker, D., Jones, S. M., Yen, A., Clark, B. C., Gamber, T., Goreva, J., Minitti, M., Sharp, T., Thornton, J. M., Willcockson, B., Zolensky, M., and Leshin, L. A., "Investigating the Use of Aerogel Collectors for the SCIM Martian-Dust Sample Return," *Lunar and Planetary Institute Science Conference Abstracts*, edited by S. Mackwell and E. Stansbery, Vol. 34 of *Lunar and Planetary Institute Science Conference Abstracts*, March 2003, pp. 1703–+.
5. Ozawa, T., Suzuki, T., Takayanagi, H., and Fujita, K., "Modeling of Martian Dust Collection for Non-stop Mars Sample Return Mission," AIAA paper 2010-0886, 48th AIAA Aerospace Sciences Meeting Including the New Horizons Forum and Aerospace Exposition, Orlando, Florida, Jan. 4-7, 2010, Jan. 2010.
6. Conrath, B. J., "Thermal Structure of the Martian Atmosphere during the Dissipation of the Dust Storm of 1971," *Icarus*, Vol. 24, 1975, pp. 36–46.
7. Bird, G. A., *Molecular Gas Dynamics and the Direct Simulation of Gas Flows*, Clarendon, Oxford, England, U.K., 1994.
8. Takayanagi, H., Suzuki, T., and Fujita, K., "Feasibility Assessment of Nonstop Mars Sample Return System," AIAA paper 2010-0627, 48th AIAA Aerospace Sciences Meeting and Exhibit, Orlando, FL, Jan 4-7, Jan. 2010.
9. Kavanau, L. L., "Heat Transfer from Spheres to a Rarefied Gas in Subsonic Flow," *ASME Trans.*, Vol. 77, No. 5, 1955, pp. 617–623.
10. Koshmarov, Y. A. and Svirshevskii, S. B., "Heat Transfer from a Sphere in the Intermediate Dynamics Region of a Rarefied Gas," *Fluid Dynamics*, Vol. 7, No. 2, 1972, pp. 343–346.
11. Sauer, F. M., "Convective Heat Transfer from Spheres in a Free-Molecule Flow," *Journal of the Aeronautical Sciences*, Vol. 18, No. 5, 1951, pp. 353–354.
12. Crowe, C. T., "Drag Coefficient of Particles in a Rocket Nozzle," *AIAA Journal*, Vol. 5, No. 5, 1967, pp. 1021–1022.
13. Melosh, H. J. and Goldin, T. J., "Heat and Drag Coefficients for Reentry of Impact Ejecta," *Lunar and Planetary Institute Science Conference Abstracts*, Vol. 39 of *Lunar and Planetary Institute Science Conference Abstracts*, March 2008, pp. 2457–+.
14. Fujita, K., Sumi, T., Yamada, T., and Ishii, N., "Heating Environments of a Venus Entry Capsule in a Trail Baloon Mission," *Journal of Thermophysics and Heat Transfer*, Vol. 20, No. 3, 2006, pp. 507–516.
15. Ozawa, T., Suzuki, T., and Fujita, K., "Experimental and Numerical Studies of Hypersonic Flows in the Rarefied Wind Tunnel," AIAA paper 2010-4513, 10th AIAA/ASME Joint Thermophysics and Heat Transfer, Chicago, Illinois, June 28-July 1, 2010, June 2010.

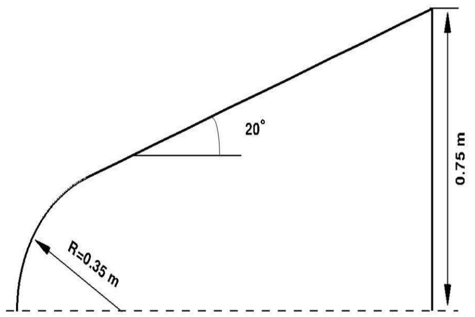

FIGURE 1. Geometry of Mars entry vehicle.

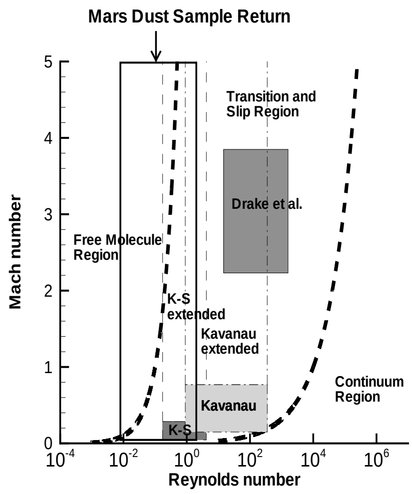

FIGURE 2. Flow regions of gas dynamics and a flow region for the Mars dust sample collection.

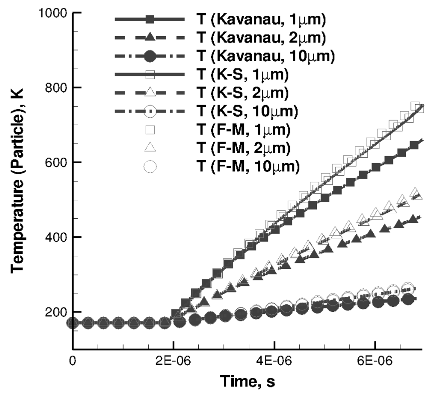

FIGURE 3. Particle temperature change using the Mars atmosphere entry flow field at 35 km with thermal decomposition.

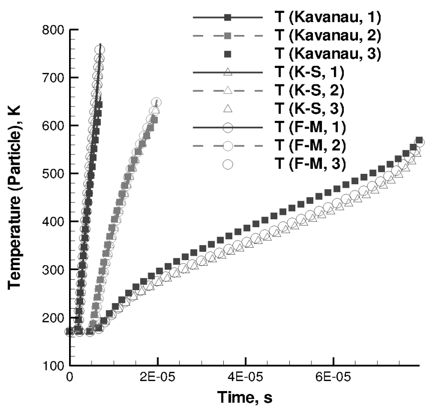

FIGURE 4. Particle (1-μm) temperature change from three different initial locations ($r = 0$, 30 and 50 cm) using the Mars atmosphere entry flow field at 35 km with thermal decomposition.

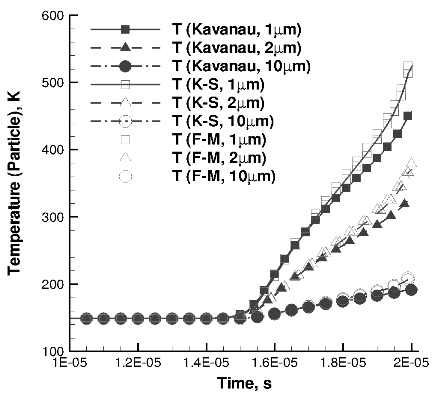

FIGURE 5. Particle temperature change using the Mars atmosphere entry flow field at 45 km with thermal decomposition.